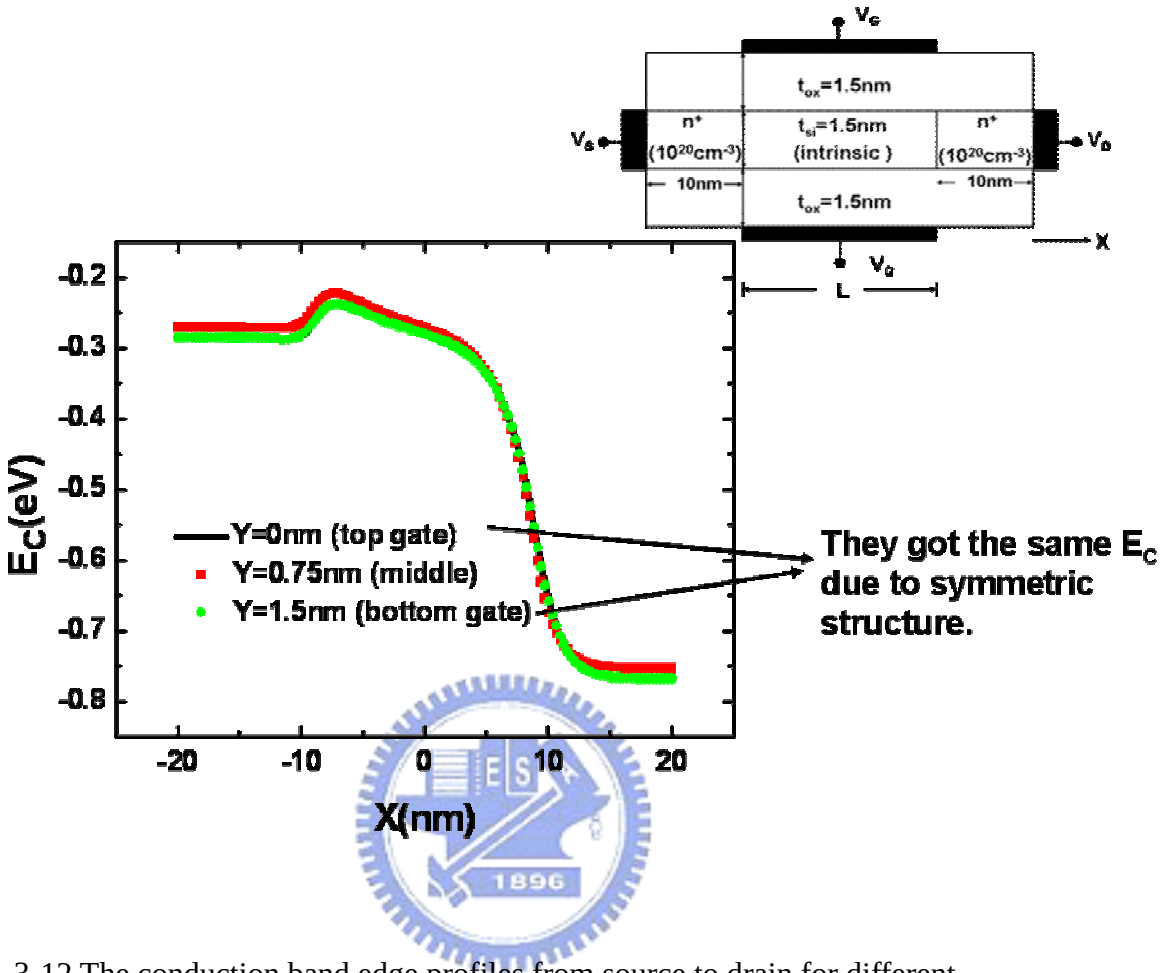

Fig. 3-12 The conduction band edge profiles from source to drain for different positions along the y direction. L=20nm.

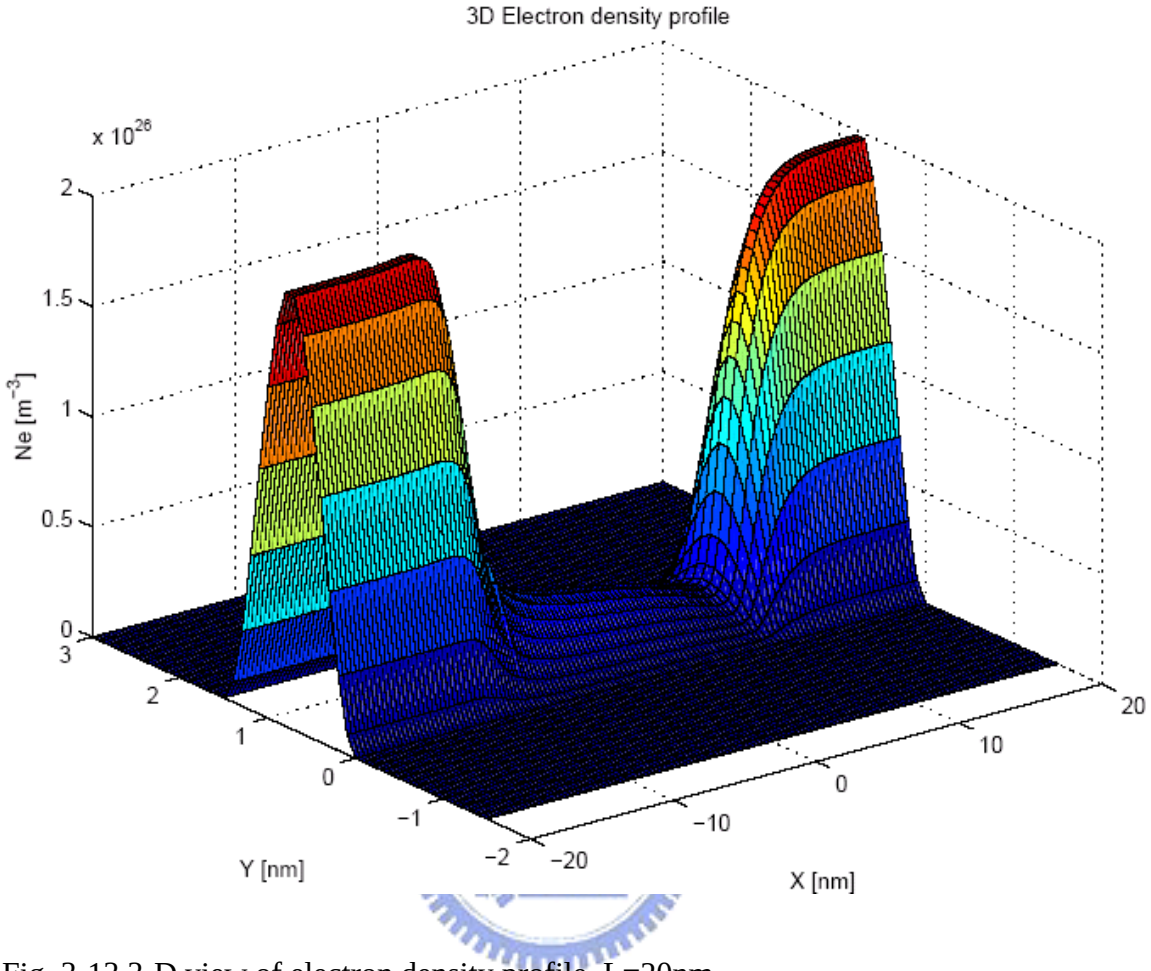

Fig. 3-13 3-D view of electron density profile. L=20nm.

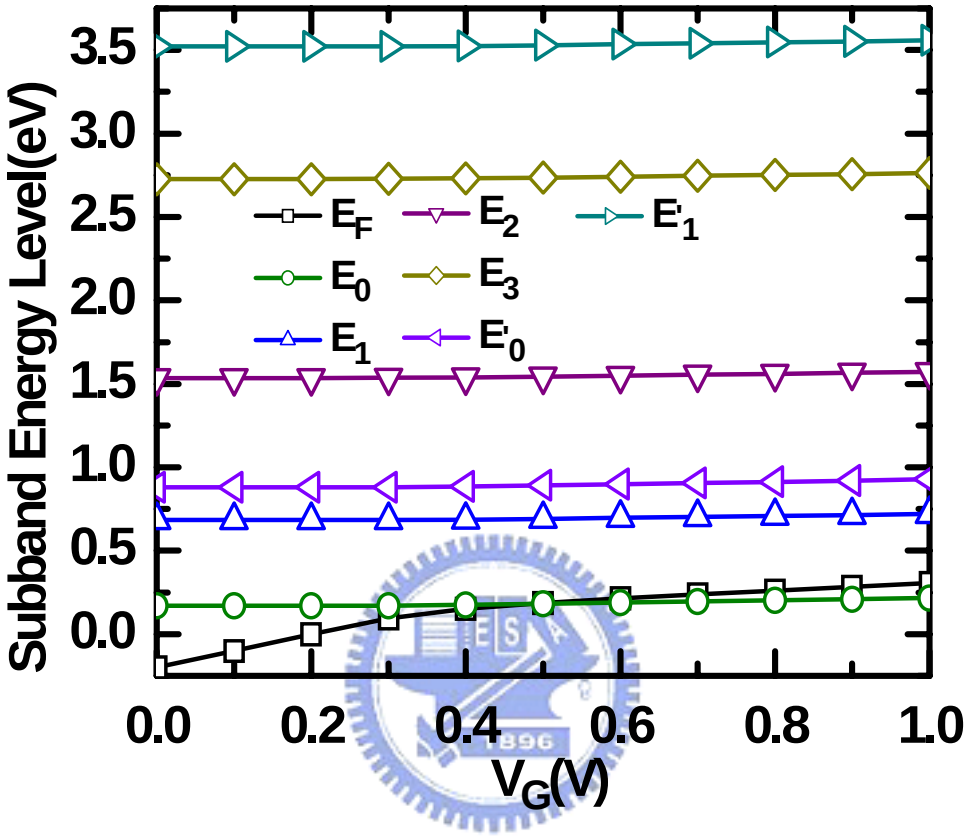

Fig. 4-1 Channel subband levels and Fermi level versus gate voltage obtained from 1-D self-consistent Schrödinger-Poisson simulation.

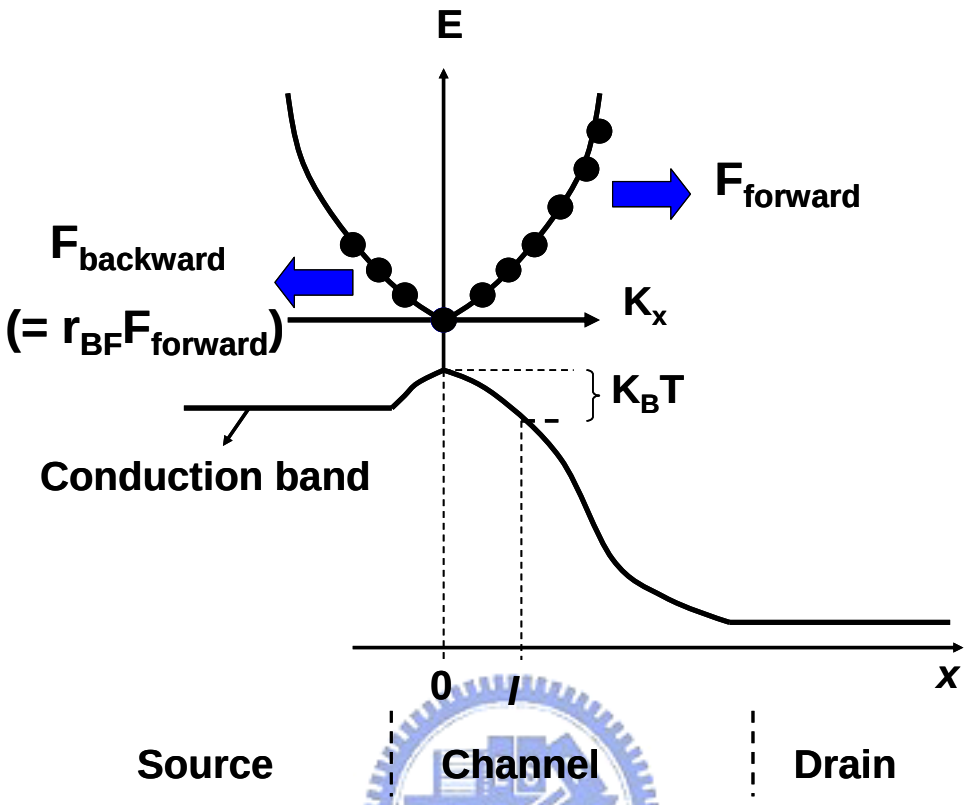

Fig. 4-2 Schematic conduction-band profile from source to drain. An E-K diagram is plotted showing forward and backward flux at the peak of the source-channel barrier.

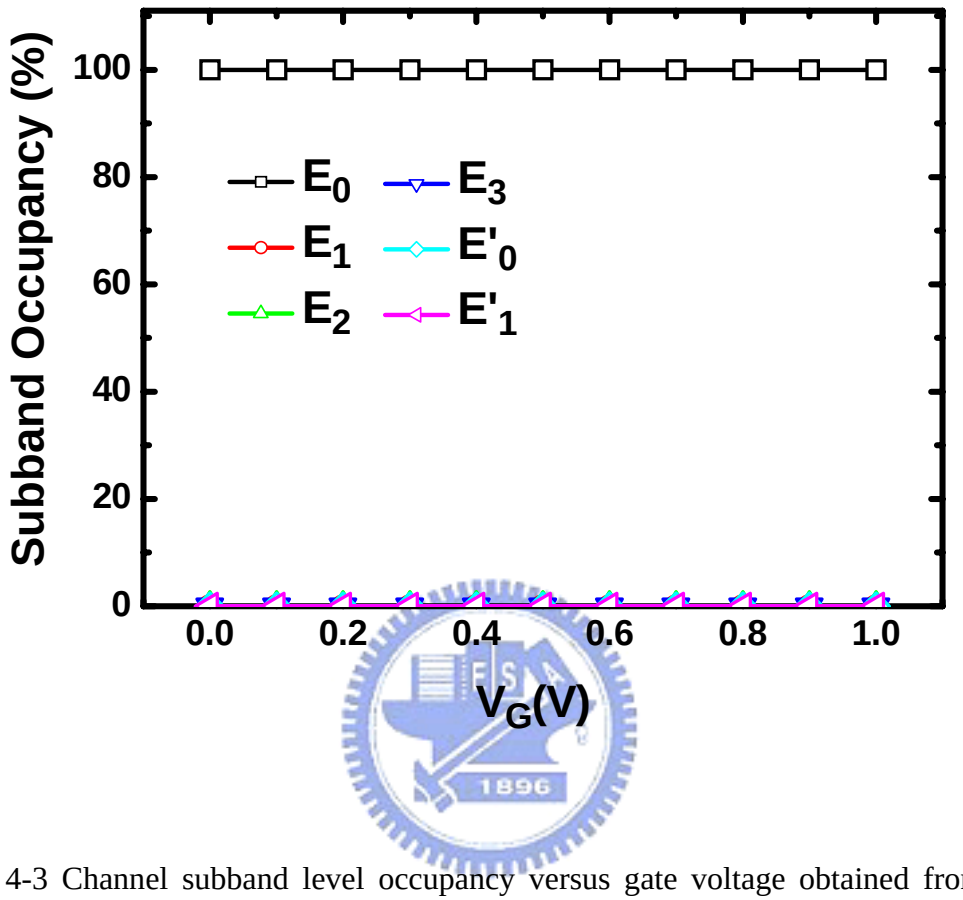

Fig. 4-3 Channel subband level occupancy versus gate voltage obtained from 1-D self-consistent Schrödinger-Poisson simulation.

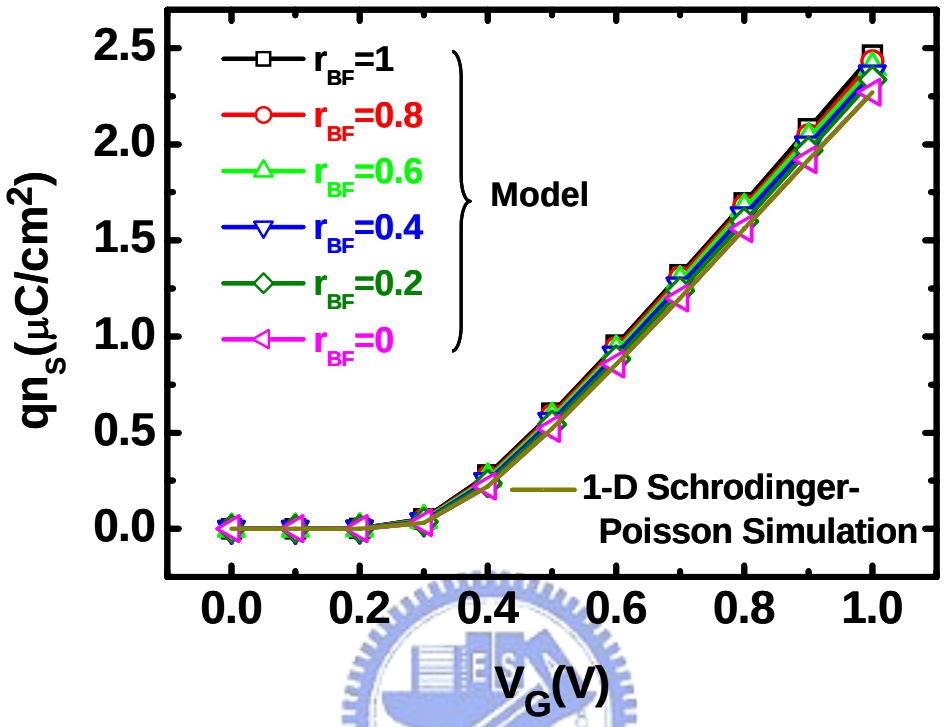

Fig. 4-4 Comparison of calculated inversion-layer charge versus gate voltage for different r_{BF} with equilibrium value (r_{BF} =1) from Schrödinger-Poisson simulation.

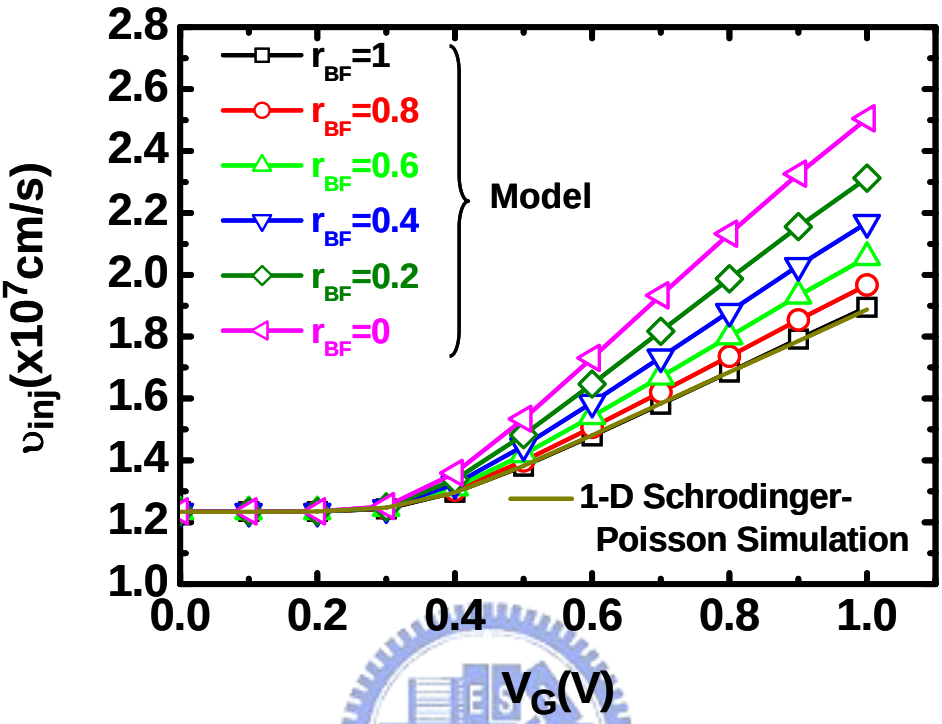

Fig. 4-5 Comparison of calculated thermal injection velocity versus gate voltage for different r_{BF} with equilibrium value (r_{BF} =1) from Schrödinger-Poisson simulation.

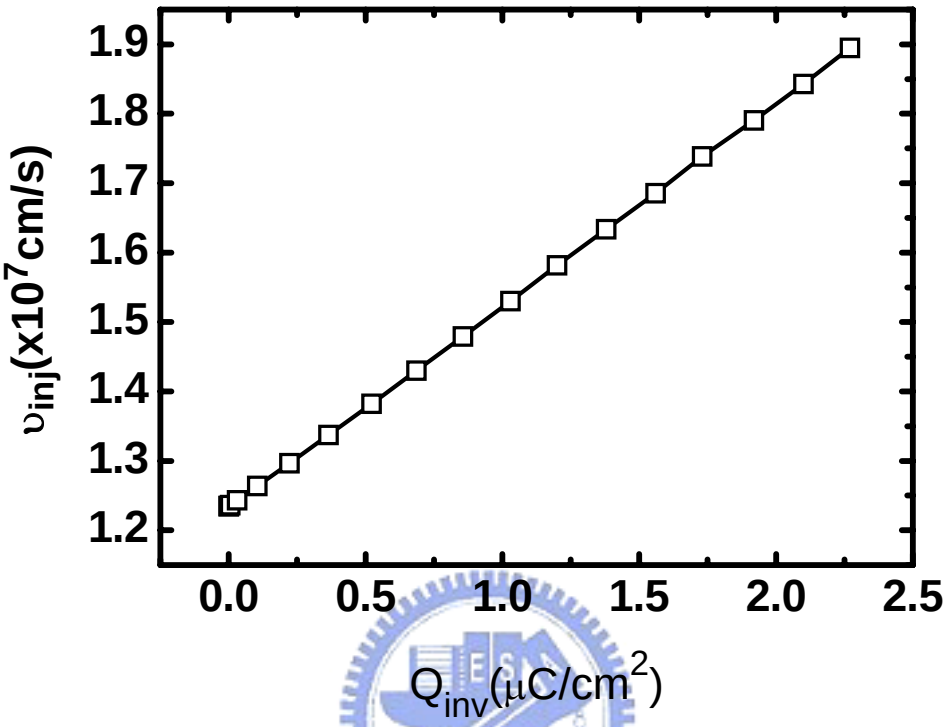

Fig. 4-6 Thermal injection velocity versus inversion-layer charge from Schrödinger - Poisson simulation.

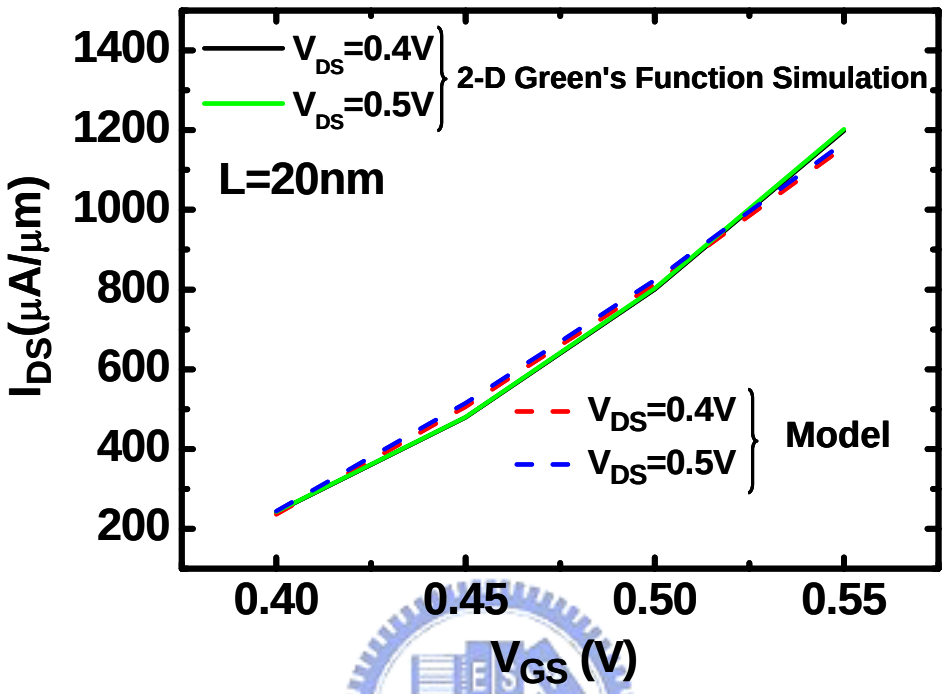

Fig. 4-7 Comparison of calculated ballistic drain current versus gate voltage for two drain voltages with those from 2-D Green's function simulation. L= 20 nm.

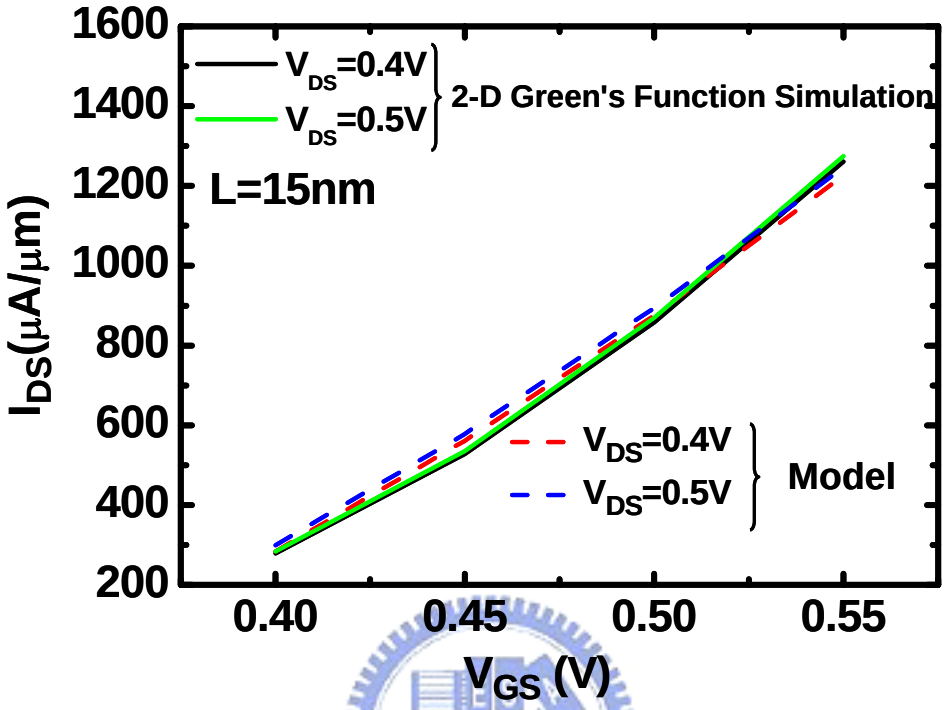

Fig. 4-8 Comparison of calculated ballistic drain current versus gate voltage for two drain voltages with those from 2-D Green's function simulation. L= 15 nm.

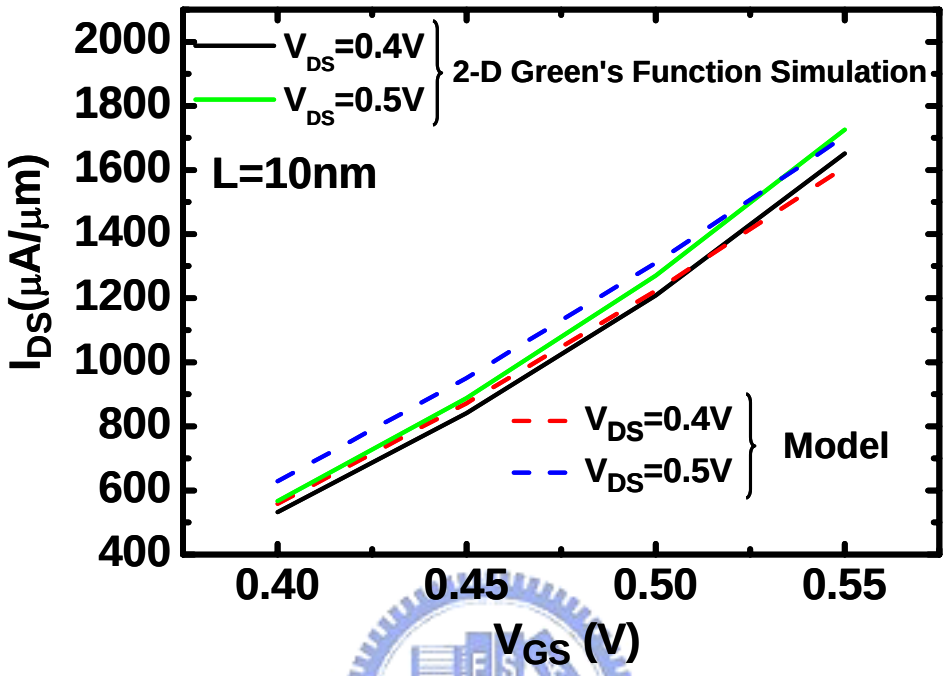

Fig. 4-9 Comparison of calculated ballistic drain current versus gate voltage for two drain voltages with those from 2-D Green's function simulation. L= 10 nm.

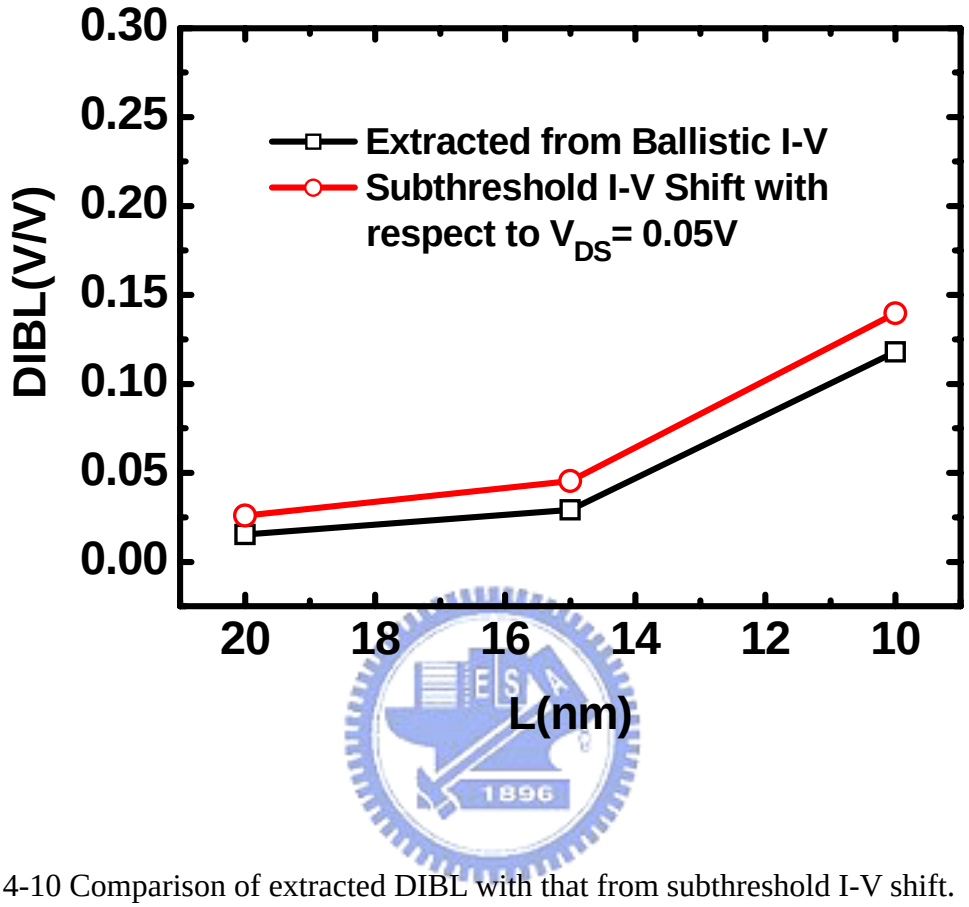

Fig. 4-10 Comparison of extracted DIBL with that from subthreshold I-V shift.

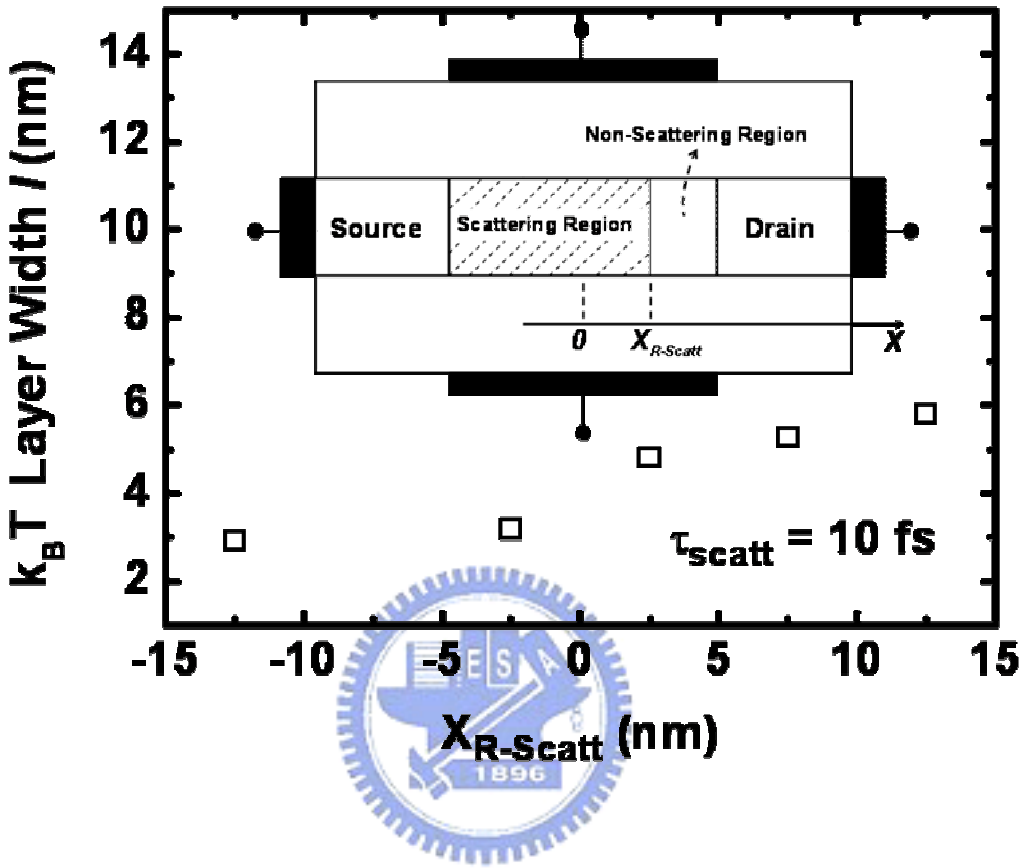

Fig. 4-11 k_BT layer width versus $X_{R\text{-}Scatt}$ as quoted from [4] for L = 25 nm. The inset shows the definition of $X_{R\text{-}Scatt}$.

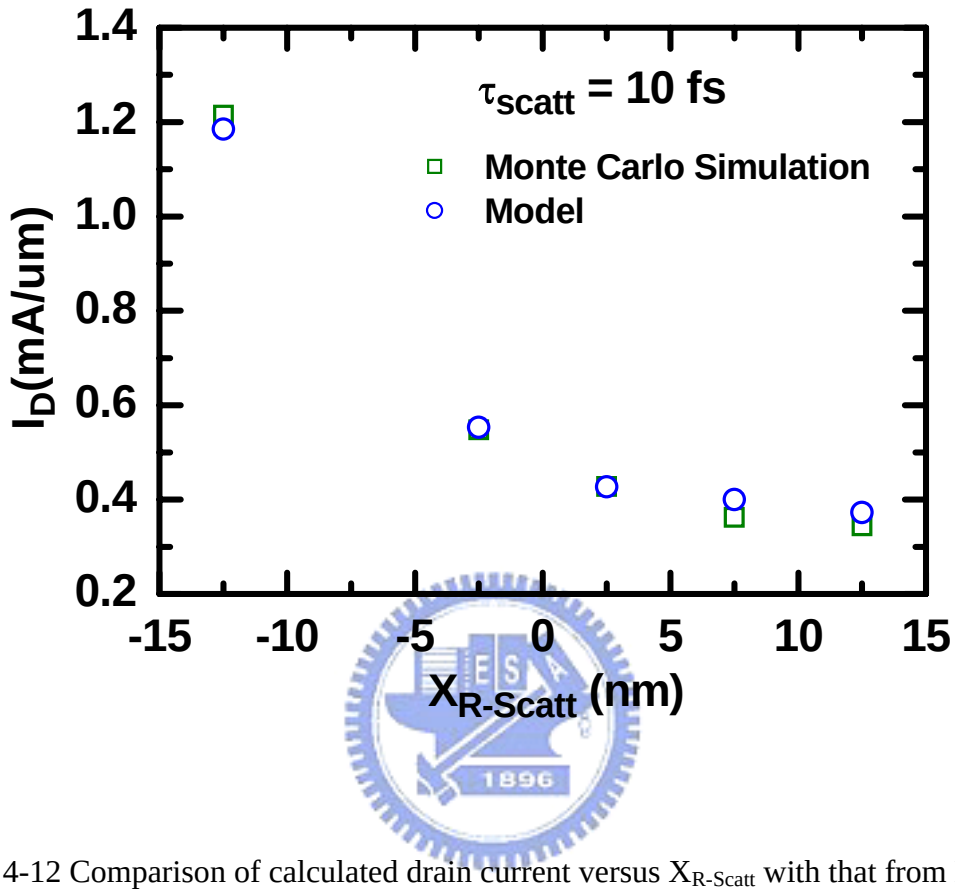

Fig. 4-12 Comparison of calculated drain current versus $X_{R\text{-}Scatt}$ with that from Monte Carlo simulation.

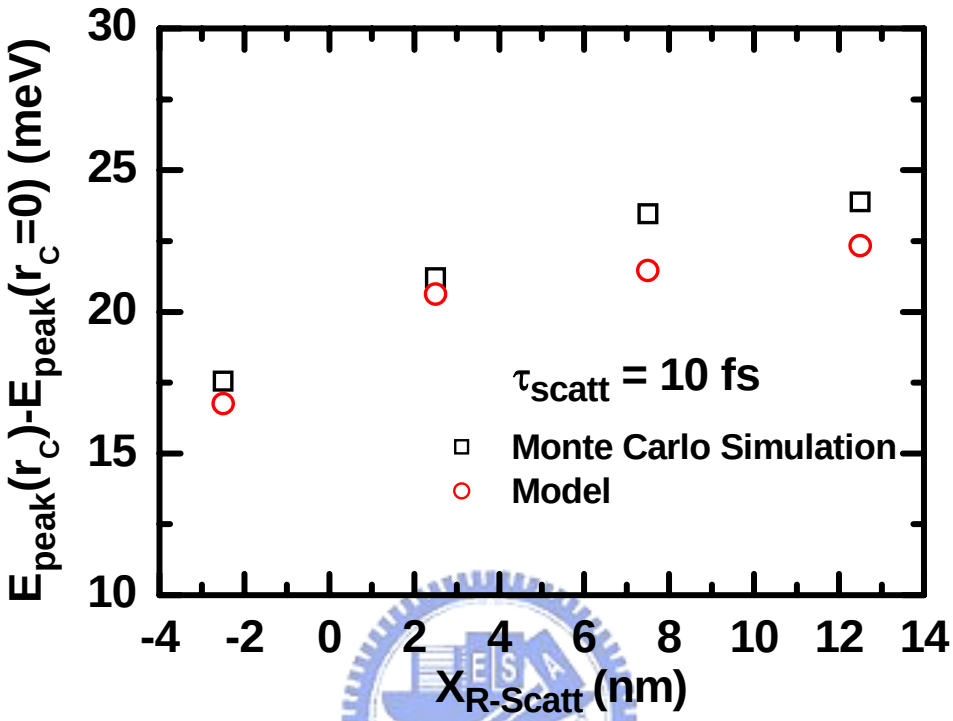

Fig. 4-13 Comparison of calculated and simulated difference in the peak of the source-channel barrier with respect to the ballistic case.

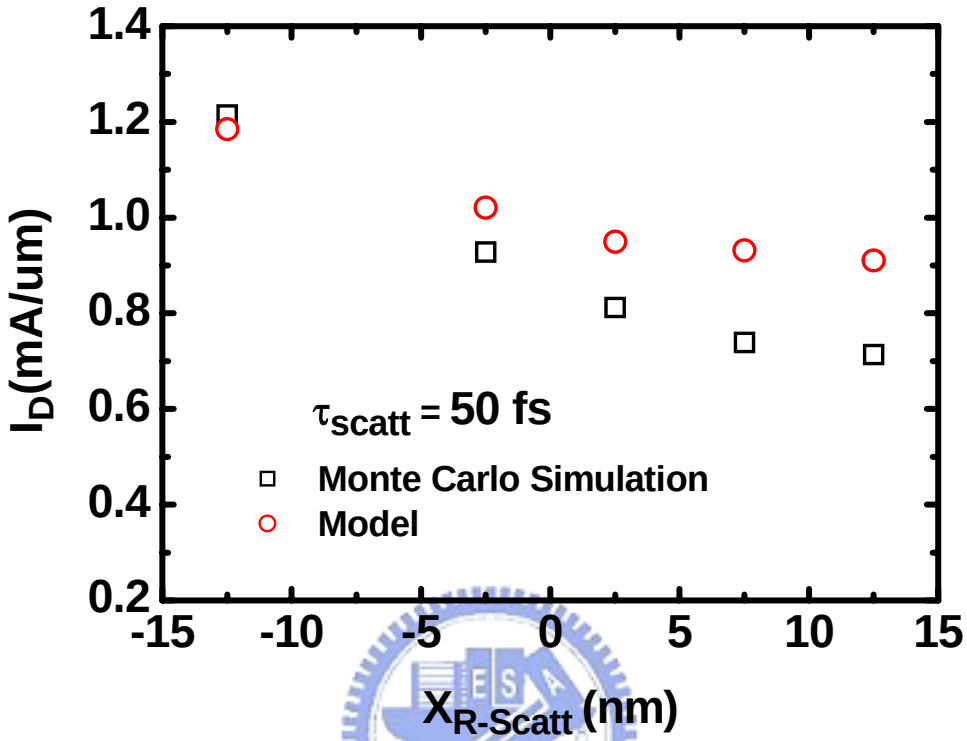

Fig. 4-14 Comparison of calculated drain current versus $X_{R\text{-}Scatt}$ with that from Monte Carlo simulation.

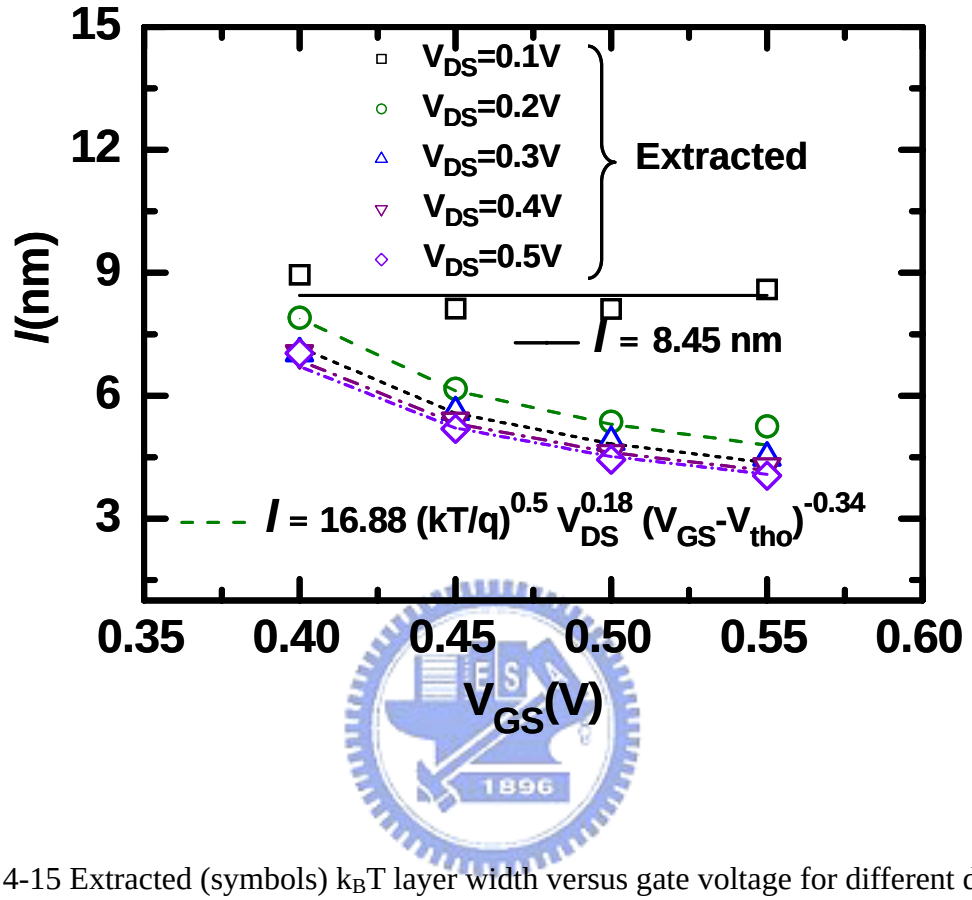

Fig. 4-15 Extracted (symbols) k_BT layer width versus gate voltage for different drain voltages. The lines are from the k_BT layer width expression.

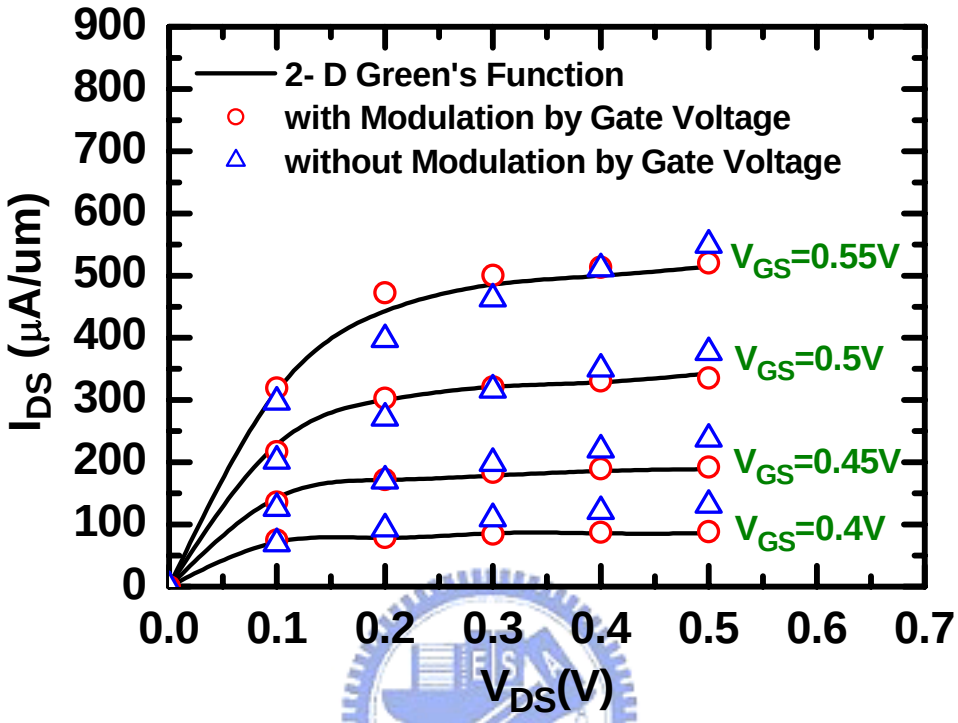

Fig.4-16 Comparison of simulated output I-V characteristics with those from compact model with and without the modulation by gate voltage. L = 20 nm.